

Preparation of a Poly-nanocage Dynamer: Correlating the Growth of Polymer Strands Using Constitutional Dynamic Chemistry and Heteroleptic Aggregation

Jian Fan,^{†,§} Manik Lal Saha,^{†,§} Bo Song,[‡] Holger Schönherr,[‡] and Michael Schmittel^{*,†}

[†]Center of Micro and Nanochemistry and Engineering, Organische Chemie I, and [‡]Physical Chemistry I, Universität Siegen, Adolf-Reichwein-Strasse 2, D-57068 Siegen, Germany

S Supporting Information

ABSTRACT: A metallocupramolecular prismatic nanocage with altogether six reactive aldehyde terminals was utilized as a sophisticated “monomer” in a template-directed constitutional dynamic imine polymerization to prepare an unprecedented triple-stranded dynamer. To analyze the correlated growth in its three congener strands, a fully covalent triple-armed star polymer was fabricated from the metallodynamer through capping, imine reduction, and removal of the template. Atomic force microscopy analysis of 68 triple-armed star polymer molecules suggests that the growth of their arms is correlated to ~72%.

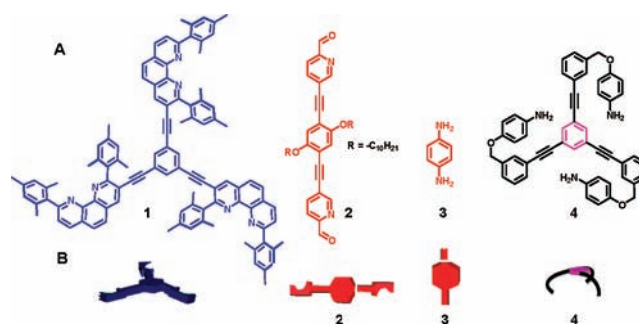
In recent years, dynamic polymers (dynamers)¹ have received much attention because of their potential for applications² in photovoltaic materials, optical limiters, chemosensors, porous membranes, etc. As monomeric units in dynamers are connected through either labile non-covalent interactions or reversible covalent bonds, the lability of the dynamic polymer strand is central to its properties, making it an adaptive material potentially responsive to changes of pH, heat, light, and even the concentration of components.³ Being alert to chemical and physical stimuli,⁴ these “smart” materials are often highly superior to traditional covalent polymers. For example, a unique key property is “self-healing”, i.e. the potential of repairing structural defects through exchange and reshuffling of components under the guidance of the thermodynamics of the global system.⁵

Until now, various types of non-covalent interactions, such as multiple hydrogen bonding,⁶ crown ether/organic salt bridge interactions,⁷ metal–ligand interactions,⁸ cyclodextrin-based hydrophilic/hydrophobic interactions,⁹ nucleobase pair interactions,¹⁰ and π – π stacking,¹¹ have been used to prepare dynamers. Metallodynamers, in which the monomers are linked through labile metal–ligand interactions, represent a highly interesting class among the various dynamic polymers because of their distinct photophysical, electrochemical, and magnetic properties.^{8b} Metal–ligand binding has also been used in combination with another weak interaction, such as hydrogen bonding, reversible covalent bond formation, and even ion pairing, for the “orthogonal” fabrication of dynamers.¹² Clearly, such copolymers not only increase the diversity of supramolecular polymers but provide access to unusual and improved properties.^{12a–c} In spite of these fascinating proper-

ties, the exploration and conceptual design of metallodynamers are still at an early stage.

At present, the most common synthetic protocol to access single-stranded metallodynamers is based on linking either difunctionalized ligands or oligomers via homoleptic metal complexation.¹² As an outstanding exception, double strands have been prepared by Yashima by metal-induced polymerization of an organic ion pair.¹³ Herein, we will report not only on an unprecedented triple-stranded metallodynamer but also on a protocol allowing all strands to grow parallel with high fidelity due to template control and cooperative effects arising from the use of a supramolecular trigonal nanocage as a sophisticated “monomer”. The ligands used are shown in Chart 1.

Chart 1. (A) Ligands 1–4 Used in the Present Study and (B) Their Cartoon Representations



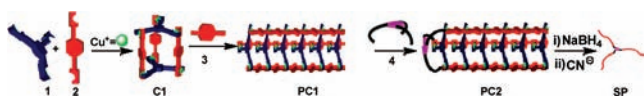
1. Alternatively, the same process may be effected without the need to pre-assemble the nanocage monomer, by mixing all constituents of the final metallodynamer. We coin this process a *template-directed constitutional dynamic polymerization* (TD-CDP) (Scheme 1). To verify correlated growth in all three strands, we have reacted the resultant dynamer at one end with a tritopic cap. After reduction of all constitutionally dynamic linkages and removal of the metal template, a fully covalent star polymer was obtained, for which atomic force microscopy (AFM) analysis showed the length of the congener arms to be strongly correlated.

At the heart of our TD-CDP approach we conceived the supramolecular prismatic nanocage **C1** as the monomer. **C1** furnishes six reactive aldehyde terminals that are perfectly

Received: October 20, 2011

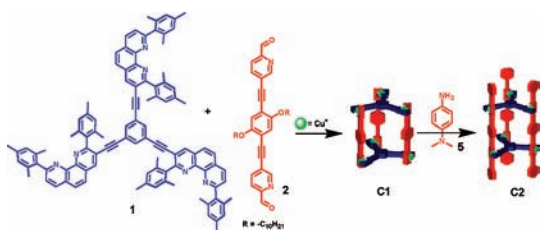
Published: December 12, 2011

Scheme 1. Cartoon Representation of the TD-CDP Approach



suiting for constitutionally dynamic imine bond formation in the presence of suitable amines.¹⁴ As described earlier, **C1** was prepared from two trisphenanthroline panels **1**, three bis-(pyridylcarbaldehyde) pillars **2**, and six Cu^+ ions (Schemes 1 and 2).¹⁵ To demonstrate that the six terminal aldehydes of **C1**

Scheme 2. Synthesis of the Prismatic Nanocage **C1** and Its Post-self-assembly Functionalization to **C2**



are readily available for imine bond formation with an electron-rich diamine as required for the TD-CDP, it was reacted with *N,N*-dimethyl-*p*-phenylenediamine (**5**). As we expected, the post-self-assembly functionalization¹⁶ of **C1** furnished quantitatively nanocage **C2** with six constitutionally dynamic imine sites (Scheme 2). Its clean formation was confirmed by ¹H NMR, ESI-MS, ¹H-¹H COSY, diffusion-ordered spectroscopy (DOSY), UV-vis, IR, and elemental analysis (Supporting Information (SI)). For example, the ESI-MS spectra exhibit three major peaks that are in full agreement with the newly formed nanocage **C2**, i.e., at 970.5, 1193.5, and 1528.0 Da, representing $[\text{Cu}_6(\mathbf{1})_2(\mathbf{9})_3]^{6+}$, $[\text{Cu}_6(\mathbf{1})_2(\mathbf{9})_3]\text{PF}_6^{5+}$, and $[\text{Cu}_6(\mathbf{1})_2(\mathbf{9})_3](\text{PF}_6)_2^{4+}$, respectively (SI, Figure S8).

To prepare the poly-nanocage dynamer **PC1** (Scheme 1), we reacted “monomer” **C1** with *p*-phenylenediamine (**3**) as a difunctionalized amine. To this end, a mixture of 1 equiv of **C1** and 3 equiv of **3** was refluxed in DCM/acetonitrile for 3 days, and the resultant red **PC1** was characterized without any further purification by ¹H NMR, DOSY NMR, IR, UV-vis spectroscopy, dynamic light scattering (DLS), transmission electron microscopy (TEM), and AFM.

While the ¹H NMR of the resultant **PC1** is mostly congruent with that of model nanocage **C2**, the broadness of the ¹H NMR signals appears typical for a polymer. Despite the broad signals, the ¹H NMR spectrum is well suited for determining the average degree of polymerization (DP) and the molecular weight of **PC1**. A comparison of the integration of the remaining aldehyde proton signal at $\delta = 9.54$ ppm¹⁵ with that of the OCH_2 protons of the $\text{OC}_{10}\text{H}_{21}$ chains at $\delta = 3.93$ ppm (cf. in **C2**: $\delta = 3.95$ ppm) suggests an average DP of 11 for each strand of the polymer (SI, Figure S11).^{12d} The average molecular weight of **PC1** thus amounts to $M_n \approx 81$ kDa and the average strand length to 33 nm, according to MM⁺ calculations (SI, Figure S22).

Formation of the metalloglycyl dimer is also supported through the results of DOSY NMR experiments. The diffusion constants *D* for both **C2** and **PC1** were measured by pulsed field gradient NMR experiments in CD_2Cl_2 using the BPPSTE pulse sequence. For the supramolecular polymer **PC1**, $D = 3.1$

$\times 10^{-11} \text{ m}^2 \text{ s}^{-1}$,^{12c,13} while a 10-fold higher value emerges with $D = 4.2 \times 10^{-10} \text{ m}^2 \text{ s}^{-1}$ for **C2** as a representative monomer.¹⁵ Furthermore, the DLS data for **PC1** show a monomodal size distribution with a hydrodynamic radius $R_H = 5.1$ nm (SI, Figure S19). In line with other reports in the literature,¹³ R_H is much smaller than the dimensions of the expected rod-like oligomers, as R_H assumes a spherical shape.

Polyimine formation at the Cu^+ binding sites in dynamer **PC1** is also readily ascertained by its diagnostic UV-vis absorptions. Whereas model cage **C2** shows two strong absorptions at 338 and 502 nm, the corresponding bands in **PC1** show up at 345 and 467 nm (SI, Figure S13). The first band in each case is assigned to an intraligand (IL) $\pi-\pi^*$ transition,^{12d} while the second one is due to metal-to-ligand charge transfer (MLCT) at the heteroleptic copper phenanthroline iminopyridine complex. It is interesting to note that in **PC1** a bathochromic shift of $\Delta\lambda = 7$ nm was observed for the $\pi-\pi^*$ absorption ($\lambda = 345$ nm) in comparison to **C2**, pointing toward extension of the π -conjugation in the polyiminopyridine strands. In contrast, the MLCT transition of **PC1** at 467 nm is markedly hypsochromically shifted by 35 nm when compared to that of **C2**, readily explainable by the transformation of a donor ($-\text{NMe}_2$) into an acceptor ($=\text{NR}$) group at the *para* position of the phenylene linkage. The imine linkages in **PC1** are additionally corroborated by IR, as the metalloglycyl dimer shows an absorption at 1581 cm^{-1} for the $\text{C}=\text{N}$ stretching vibration, while **C2** shows one at 1585 cm^{-1} .

So far, any attempt to characterize more accurately the average molecular weight of **PC1** by gel permeation chromatography (GPC) was met with failure because of its poor solubility. Fortunately, direct evidence for the nanorod structure of the metalloglycyl dimer **PC1** was obtained by AFM and TEM analysis (Figures 1 and S20 in SI, respectively). A

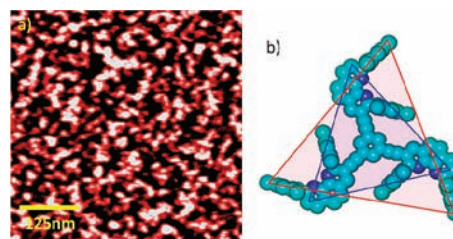


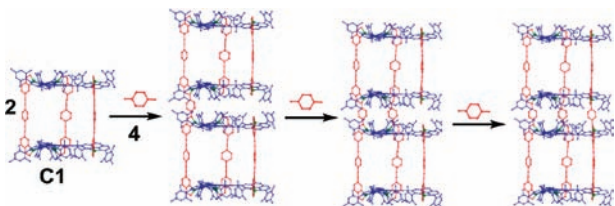
Figure 1. (a) AFM height image of metalloglycyl dimer **PC1**. (b) Hyperchem structure of **1**. Carbon, cyan; nitrogen, blue; hydrogen, not shown. The height of the blue triangle is 1.81 nm, and that of the red triangle is 2.33 nm.

disordered arrangement of polymer strands of varying length is seen (Figure 1a). The rod-like structures possess an apparent height of 2.4 nm (SI, Figure S17), which is in full agreement with the result from an MM⁺ simulation. The height and width of the metalloglycyl dimer can be best approximated by the size of trisphenanthroline **1** using the inner blue triangle (height = 1.81 nm) with vertices defined by the phenanthroline atoms farthest from the central benzene. The outer triangle (height = 2.33 nm) with vertices defined by the outer-most mesitylene atoms (red) defines only the trisphenanthroline **1** itself but not the polyimine strands (Figure 1b).

A battery of experimental evidence thus asserts that the trisphenanthroline building blocks **1** and the polyiminopyridine strands in **PC1** are organized in a highly defined manner via heteroleptic complexation as guided by the HETPHEN

methodology.¹⁷ During polymerization, the Cu^+ ions in **C1** catalyze the polyimine formation and eventually bind the growing strands as ligands. Due to cooperative effects, the parallel growth in the three congener strands of **PC1** ought to be guaranteed. In detail, once any arbitrary polymer chain has grown by one unit, “strand 1” will preorganize the template such that the second and third strands will profit from cooperative effects in their elongation (Scheme 3). Therefore,

Scheme 3. Illustration of the TD-CDP Approach in the Dimerization of **C1** with **3**



due to the dynamic heteroleptic coordination at the terminus of the growing polymer, the tris(phenanthroline- Cu^+) unit will support the parallel growth of three polymer strands. To correlate the growth in all three congener strands in **PC1**, both the covalent imine bonds and the heteroleptic complexes need to be fully reversible in order to allow for error correction in the TD-CDP. In principle, chain growth may stall anywhere along its extension while maintaining coordination of the tris(phenanthroline- Cu^+) unit to the pyridylaldehyde terminal. Comparison of binding constants, however, reveals that the electron-rich (*p*- NMe_2 -substituted) iminopyridine is a better chelate ligand ($\text{N}_{\text{py}}=\text{C}_{\text{py}}-\text{C}=\text{N}$) for copper(I) phenanthrolines ($\log K = 6.15 \pm 0.21$) than the corresponding pyridylaldehyde ($\text{N}_{\text{py}}=\text{C}_{\text{py}}-\text{C}=\text{O}$, $\log K = 3.83 \pm 0.35$) (SI, Figures S14 and S15).

So far, the experimental data clearly support the formation of **PC1** but do not allow an evaluation of the amount of defects along the triple-chain aggregate. To quantify the amount of defect-free correlated growth, we thus decided to transform the triple-stranded dynamer **PC1** into the covalent triple-armed star polymer **SP** and to interrogate its arm lengths (Scheme 1, last two steps).

We showed earlier that **C1** can be transformed into a doubly capped cage-like 3D framework by reacting 1 equiv of **C1** with 2 equiv of the tritopic end-cap **4**.¹⁵ Along the same line, we expected that in presence of only 1 equiv of **4**, **C1** may provide a monocapped nanocage structure. Indeed, formation of the monocapped nanocage was confirmed by ESI-MS data (SI, Figure S9). Similarly, the metallodynamer **PC1** provides reactive aldehyde terminals that could be used for a capping reaction at one terminus of the dynamer strand. Thus, **PC1** was refluxed with 0.02 equiv of **3** (related to the initial amount of **C1**) in a DCM/acetonitrile mixture for 3 days. An ensuing reduction of all imine units with NaBH_4 kinetically locked the capped polymer, and finally demetalation with aqueous sodium cyanide liberated polymer **SP** from the supramolecular scaffold (Scheme 1). To our delight, subsequent examination of the covalent **SP** by AFM verified its star-like triple-armed structure (Figure 2a and also SI, Figure S18). Figure 2b shows the average arm lengths for a total of 68 triple-armed star molecules (SI, Table S2). Most of the star-shaped polymers show an arm length from 20 to 35 nm. The histogram provides an arm-length distribution ranging from 10 to 50 nm, with an average

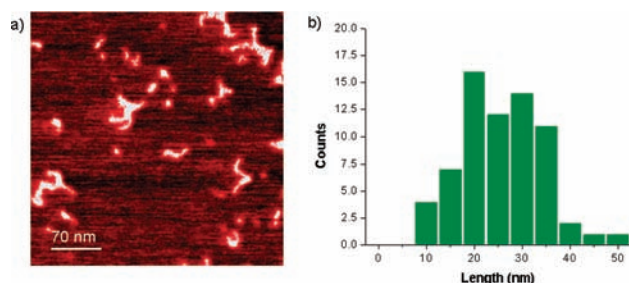


Figure 2. (a) AFM phase image of star polymer **SP**. (b) The histogram represents the average arm length distribution for **SP**.

arm length of ~ 26 nm, corresponding to a molecular weight of 22 kDa that is in good agreement with the average molecular weight determined from GPC analysis (20 kDa, SI, Figure S21).

For practical reasons, we have estimated the error in the arm-length assessment. It seemed reasonable to use an error margin of ± 6 nm (3 nm corresponds to the length of one monomer unit); i.e., any two arms will be judged as of the same length if their length difference as measured by AFM is not larger than 6 nm. Among 68 investigated star molecules, 72% of the molecules (49 molecules) show correlated growth in their polymer chains within the error limit (SI, Table S2). Among the correlated examples, 39 molecules are doubly correlated; i.e., two strands are of equal length within the error limit, and 10 molecules are triply correlated. Notably, among the latter 10 examples, three have an average arm length of 35 nm.

According to our assessment, the high correlation in the arm lengths nicely reflects the correlated triple-stranded growth of **PC1** via reversible and cooperative imine formation at the Cu^+ phenanthroline termini (Scheme 3). However, the transformation of the dynamer **PC1** into the covalent star polymer **SP** with three arms of the same length requires a high fidelity not only in the polymer growth but equally in the imine reduction step. Clearly, any imine bond left untouched in the NaBH_4 reduction would be hydrolyzed in the aqueous demetalation workup, thus generating one arm that is uncorrelated in length with the two others. The finding of star polymers with only two arms correlated in length indicates that some of the imine bonds are not reduced and thus are hydrolyzed in the demetalation step. Clearly, with increasing arm length of a star molecule, the probability of finding non-correlated arm lengths should be increased. For example, the finding of a star molecule with three arms of 26 nm length requires to produce and to reduce ~ 60 imine bonds with high fidelity, indicating that a total of 120 reactions must work out at 100%. For the triply correlated star molecule with an average arm length of 35 nm, ~ 160 reactions need to work at 100% fidelity.

Another important message is that our length assessment of the dynamic polymer **PC1** ($DP = 11$) based on end group analysis is consistent with that of the covalent star polymer **SP** determined by AFM ($DP = 10$). This agreement provides indirect support that there are not many defects in the dynamic polymer **PC1**, as inner and terminal aldehyde units would contribute to the end group analysis.

The claim of correlated growth requires that the doubly and triply correlated star polymer molecules form in an amount far above their statistical weight. In order to estimate the percentage of correlated star molecules expected by statistical analysis, we should consider a suitable theoretical model that

fits our system. Since the mechanism basically relies on a polycondensation, one expects the distribution to follow Flory's statistics.¹⁸ However, the precise representation of our complicated system in Flory's model is a cumbersome. Nevertheless, to get some educated guess, we calculated the expected distribution data if correlated growth would not apply. A simple statistical estimate of uncorrelated growth in a triple-armed star polymer suggests that only 3% of those molecules would be triply correlated and 13% would be doubly correlated. Clearly, the system is not guided by statistical control (SI, page S24).

In conclusion, the TD-CDP approach, due to its inherent template control and cooperative effects, provides an elegant route for the preparation of multi-armed polymer molecules with arms of identical length. As a demonstration of the concept, we have described the formation of the triple-stranded poly-nanocage **PC1**, in which tris(phenanthroline-Cu⁺) units and polyiminopyridines are organized in a highly defined manner via heteroleptic complexation. To the best of our knowledge, **PC1** represents the first example of a triple-stranded metallodynamer. The post-polymerization reduction of **PC1** generates a kinetically locked polyamine still affixed to a supramolecular scaffold, while subsequent demetalation liberates a triple-armed star-like polymer. AFM analysis of individual star polymer molecules suggests that the growth of their arms is correlated up to 72%. In principle, the methodology should allow the preparation of bicyclic, polycyclic, and star polymers with identical lengths of all strands or arms, with the prospect that these yet unknown polymers may convey interesting properties.

■ ASSOCIATED CONTENT

■ Supporting Information

Experimental procedures and spectroscopic data for complexes **C2** and **C5** and polymeric assemblies **PC1** and **SP** are provided. This material is available free of charge via the Internet at <http://pubs.acs.org>

■ AUTHOR INFORMATION

Corresponding Author

schmittel@chemie.uni-siegen.de

Author Contributions

[§]These authors contributed equally.

■ ACKNOWLEDGMENTS

We are indebted to the DFG, the AvH foundation (J.F. and B.S.), and the University of Siegen for financial support. We thank Dr. M. Hess (GPC analysis), Dr. D. Tranchida, Dr. S. Ma (preliminary AFM and TEM), Prof. Dr. R. Trettin (DLS), and Dr. S. Neogi (artwork in Scheme 3), all from the University of Siegen, for their support.

■ REFERENCES

- (1) (a) Brunsveld, L.; Folmer, B. J. B.; Meijer, E. W.; Sijbesma, R. P. *Chem. Rev.* **2001**, *101*, 4071. (b) Lehn, J.-M. *Prog. Polym. Sci.* **2005**, *30*, 814. (c) De Greef, T. F. A.; Meijer, E. W. *Nature* **2008**, *453*, 171. (d) De Greef, T. F. A.; Smulders, M. M. J.; Wolffs, M.; Schenning, A. P. H. J.; Sijbesma, R. P.; Meijer, E. W. *Chem. Rev.* **2009**, *109*, 5687.
- (2) (a) Hwang, S.-H.; Moorefield, C. N.; Newkome, G. R. *Chem. Soc. Rev.* **2008**, *37*, 2543. (b) Whittell, G. R.; Hager, M. D.; Schubert, U. S.; Manners, I. *Nat. Mater.* **2011**, *10*, 176. (c) Winter, A.; Hoeppeper, S.; Newkome, G. R.; Schubert, U. S. *Adv. Mater.* **2011**, *23*, 3484.

- (3) (a) Lehn, J.-M. *Chem. Soc. Rev.* **2007**, *36*, 151. (b) Ono, T.; Fujii, S.; Nobori, T.; Lehn, J.-M. *Chem. Commun.* **2007**, 46. (c) Folmer-Andersen, J. F.; Lehn, J.-M. *Angew. Chem., Int. Ed.* **2009**, *48*, 7664.

- (4) (a) Liao, X.; Chen, G.; Liu, X.; Chen, W.; Chen, F.; Jiang, M. *Angew. Chem., Int. Ed.* **2010**, *49*, 4409. (b) Guo, D.-S.; Chen, S.; Qian, H.; Zhang, H.-Q.; Liu, Y. *Chem. Commun.* **2010**, 46, 2620.

- (5) (a) Cordier, P.; Tournilhac, F.; Soulié-Ziakovic, C.; Leibler, L. *Nature* **2008**, *451*, 977. (b) Bergman, S. D.; Wudl, F. *J. Mater. Chem.* **2008**, *18*, 41. (c) Burattini, S.; Greenland, B. W.; Hermida Merino, D.; Weng, W.; Seppala, J.; Colquhoun, H. M.; Hayes, W.; Mackay, M. E.; Hamley, I. W.; Rowan, S. J. *J. Am. Chem. Soc.* **2010**, *132*, 12051.

- (6) (a) Wilson, A. J. *Soft Matter* **2007**, *3*, 409. (b) Fox, J. D.; Rowan, S. J. *Macromolecules* **2009**, *42*, 6823.

- (7) (a) Huang, F.; Gibson, H. W. *Prog. Polym. Sci.* **2005**, *30*, 982. (b) Niu, Z.; Huang, F.; Gibson, H. W. *J. Am. Chem. Soc.* **2011**, *133*, 2836. (c) Dong, S.; Luo, Y.; Yan, X.; Zheng, B.; Ding, X.; Yu, Y.; Ma, Z.; Zhao, Q.; Huang, F. *Angew. Chem., Int. Ed.* **2011**, *50*, 1905.

- (8) (a) Dobrawa, R.; Würthner, F. *J. Polym. Sci., Part A: Polym. Chem.* **2005**, *43*, 4981. (b) Han, F. S.; Higuchi, M.; Kurth, D. G. *J. Am. Chem. Soc.* **2008**, *130*, 2073. (c) Chipper, M.; Hoogenboom, R.; Schubert, U. S. *Macromol. Rapid Commun.* **2009**, *30*, 565. (d) Wang, F.; Zhang, J.; Ding, X.; Dong, S.; Liu, M.; Zheng, B.; Li, S.; Wu, L.; Yu, Y.; Gibson, H. W.; Huang, F. *Angew. Chem., Int. Ed.* **2010**, *49*, 1090.

- (9) Harada, A.; Takashima, Y.; Yamaguchi, H. *Chem. Soc. Rev.* **2009**, *38*, 875.

- (10) Sivakova, S.; Wu, J.; Campo, C. J.; Mather, P. T.; Rowan, S. J. *Chem.-Eur. J.* **2006**, *12*, 446.

- (11) Burattini, S.; Greenland, B. W.; Hayes, W.; Mackay, M. E.; Rowan, S. J.; Colquhoun, H. M. *Chem. Mater.* **2011**, *23*, 6.

- (12) (a) Hofmeier, H.; Hoogenboom, R.; Wouters, M. E. L.; Schubert, U. S. *J. Am. Chem. Soc.* **2005**, *127*, 2913. (b) Chow, C.-F.; Fujii, S.; Lehn, J.-M. *Angew. Chem., Int. Ed.* **2007**, *46*, 5007. (c) Gröger, G.; Stepanenko, V.; Würthner, F.; Schmuck, C. *Chem. Commun.* **2009**, 698. (d) de Hatten, X.; Bell, N.; Yufa, N.; Christmann, G.; Nitschke, J. R. *J. Am. Chem. Soc.* **2011**, *133*, 3158. (e) Li, S.-L.; Xiao, T.; Wu, Y.; Jiang, J.; Wang, L. *Chem. Commun.* **2011**, 47, 6903. (f) Gröger, G.; Meyer-Zaika, W.; Böttcher, C.; Gröhn, F.; Ruthard, C.; Schmuck, C. *J. Am. Chem. Soc.* **2011**, *133*, 8961. (g) Grimm, F.; Ulm, N.; Gröhn, F.; Düring, J.; Hirsch, A. *Chem.-Eur. J.* **2011**, *17*, 9478.

- (13) Ikeda, M.; Tanaka, Y.; Hasegawa, T.; Furusho, Y.; Yashima, E. *J. Am. Chem. Soc.* **2006**, *128*, 6806.

- (14) (a) Fan, J.; Bats, J. W.; Schmittel, M. *Inorg. Chem.* **2009**, *48*, 6338. (b) Granzhan, A.; Riis-Johannessen, T.; Scopelliti, R.; Severin, K. *Angew. Chem., Int. Ed.* **2010**, *49*, 5515. (c) Campbell, V. E.; de Hatten, X.; Delsuc, N.; Kauffmann, B.; Huc, I.; Nitschke, J. R. *Nat. Chem.* **2010**, *2*, 684. (d) Granzhan, A.; Schouwey, C.; Riis-Johannessen, T.; Scopelliti, R.; Severin, K. *J. Am. Chem. Soc.* **2011**, *133*, 7106.

- (15) Schmittel, M.; Saha, M. L.; Fan, J. *Org. Lett.* **2011**, *13*, 3916.

- (16) (a) Thomas, J. A. *Chem. Soc. Rev.* **2007**, *36*, 856. (b) Wang, M.; Lan, W.-J.; Zheng, Y.-R.; Cook, T. R.; White, H. S.; Stang, P. J. *J. Am. Chem. Soc.* **2011**, *133*, 10752. (c) Zheng, Y.-R.; Lan, W.-J.; Wang, M.; Cook, T. R.; Stang, P. J. *J. Am. Chem. Soc.* **2011**, *133*, 17045.

- (17) (a) Schmittel, M.; Ganz, A. *Chem. Commun.* **1997**, 999. (b) Schmittel, M.; Ganz, A.; Fenske, D.; Herderich, M. *J. Chem. Soc., Dalton Trans.* **2000**, 353.

- (18) Flory, P. J. *Principles of Polymer Chemistry*; Cornell University Press: Ithaca, NY, 1953.